Biochemical and Biophysical Research Communications 458 (2015) 843–848

Contents lists available at ScienceDirect

Biochemical and Biophysical Research Communications

journal homepage: www.elsevier.com/locate/ybbrc

Structural analysis of PseH, the *Campylobacter jejuni* N-acetyltransferase involved in bacterial O-linked glycosylation

Wan Seok Song [a], Mi Sun Nam [a, 1], Byeol Namgung [a, 1], Sung-il Yoon [a, b, *]

[a] Department of Systems Immunology, College of Biomedical Science, Kangwon National University, Chuncheon 200-701, Republic of Korea
[b] Institute of Bioscience and Biotechnology, Kangwon National University, Chuncheon 200-701, Republic of Korea

ARTICLE INFO

Article history:
Received 21 January 2015
Available online 16 February 2015

Keywords:
Campylobacter jejuni
PseH
Bacterial protein glycosylation
N-acetyltransferase
Crystal structure

ABSTRACT

Campylobacter jejuni is a bacterium that uses flagella for motility and causes worldwide acute gastroenteritis in humans. The *C. jejuni* N-acetyltransferase PseH (cjPseH) is responsible for the third step in flagellin O-linked glycosylation and plays a key role in flagellar formation and motility. cjPseH transfers an acetyl group from an acetyl donor, acetyl coenzyme A (AcCoA), to the amino group of UDP-4-amino-4,6-dideoxy-N-acetyl-β-L-altrosamine to produce UDP-2,4-diacetamido-2,4,6-trideoxy-β-L-altropyranose. To elucidate the catalytic mechanism of cjPseH, crystal structures of cjPseH alone and in complex with AcCoA were determined at 1.95 Å resolution. cjPseH folds into a single-domain structure of a central β-sheet decorated by four α-helices with two continuously connected grooves. A deep groove (groove-A) accommodates the AcCoA molecule. Interestingly, the acetyl end of AcCoA points toward an open space in a neighboring shallow groove (groove-S), which is occupied by extra electron density that potentially serves as a pseudosubstrate, suggesting that the groove-S may provide a substrate-binding site. Structure-based comparative analysis suggests that cjPseH utilizes a unique catalytic mechanism of acetylation that has not been observed in other glycosylation-associated acetyltransferases. Thus, our studies on cjPseH will provide valuable information for the design of new antibiotics to treat *C. jejuni*-induced gastroenteritis.

© 2015 Elsevier Inc. All rights reserved.

1. Introduction

Protein glycosylation has long been believed to be confined to eukaryotes [1,2]. However, it is now evident that protein glycosylation also occurs in some of bacterial species, including *Campylobacter jejuni*, *Helicobacter pylori*, *Neisseria gonorrhoeae*, *Escherichia coli*, and *Pseudomonas aeruginosa* [3]. *C. jejuni* is unique in that it possesses both N-linked glycosylation and O-linked glycosylation systems, while other bacterial species have been demonstrated to have only one of these pathways [4,5]. The *C. jejuni* genome encodes a number of enzymes for protein glycosylation. A series of Pse enzymes (PseB, PseC, PseH, PseG, and PseI for O-glycosylation) and Pgl enzymes (PglF, PglE, and PglD for N-glycosylation) produce bacteria-specific monosaccharides, pseudaminic acid and diacetamidobacillosamine, respectively, which are eventually linked to target proteins [5]. Interestingly, in both glycosylation pathways, the initial substrate is identical with the nucleotide-linked sugar UDP-N-acetylglucosamine (UDP-GlcNAc) and undergoes three similar catalytic reactions (C6 dehydration by PseB and PglF; C4 amination by PseC and PglE; 4-N-acetylation by PseH and PglD) [6–8].

C. jejuni is one of the major causative pathogens of acute gastroenteritis and the peripheral neuropathy Guillain-Barré syndrome in humans. *C. jejuni* migrates to and moves in the mucus layer of the gastrointestinal tissue by means of flagella, and thus, flagellar motility is important for colonization and a significant virulence factor in humans. The flagellar filament consists of one type of protein, flagellin, which is heavily O-glycosylated, with up to approximately 10% of its total mass by pseudaminic acid and its derivatives [9,10]. Pseudaminic acid is biosynthesized and appended to flagellin by seven Pse enzymes, including PseB, PseC, PseH, PseG, PseI, PseF, and PseE [5,8,11,12]. PseB dehydrates and epimerizes UDP-GlcNAc to UDP-2-acetamido-2,6-dideoxy-β-L-arabino-hexos-4-ulose, which is aminated to UDP-4-amino-4,6-dideoxy-N-acetyl-β-L-altrosamine by PseC. The amino sugar is acetylated by the PseH

* Corresponding author. 1 Kangwondaehak-gil, Biomedical Science building A-204, Chuncheon 200-701, Republic of Korea. Fax: +82 33 250 8380.
E-mail address: sungil@kangwon.ac.kr (S.-i. Yoon).
[1] These authors contributed equally to this work.

http://dx.doi.org/10.1016/j.bbrc.2015.02.041
0006-291X/© 2015 Elsevier Inc. All rights reserved.

acetyltransferase (Fig. S1A), and then, the UDP moiety of the acetylated product is eliminated by PseG. PseI catalyzes the condensation reaction to form pseudaminic acid. Next, pseudaminic acid is activated using CMP by PseF and covalently linked to serine or threonine residues of flagellin by PseE. In addition to *C. jejuni*, this elaborate multi-step process of seven consecutive enzymes for the O-glycosylation of flagellin is also conserved in *H. pylori*, another species of ε-proteobacteria that causes gastritis, gastric ulcer, and gastric cancer [8]. Because flagellin glycosylation by pseudaminic acid is essential for the mobility and virulence of *C. jejuni* and *H. pylori*, each of the O-linked glycosylation enzymes can provide a valuable avenue for the development of novel antibiotic therapeutics that selectively target *C. jejuni* and *H. pylori*. Moreover, bioengineering of these enzymes may provide an alternative method to produce pseudaminic acid, which has been considered as an attractive vaccine. Despite the biological and biomedical significance of bacterial O-linked glycosylation, available structural information is limited to only three enzymes (*C. jejuni* PseG, *H. pylori* PseB, and *H. pylori* PseC), and thus, O-glycosylation mechanisms are poorly understood [12–14].

PseH belongs to the GCN5-related N-acetyltransferase (GNAT) superfamily and is responsible for the third step in the pseudaminic acid biosynthesis pathway. PseH acetylates the 4-amino group of UDP-4-amino-4,6-dideoxy-N-acetyl-β-L-altrosamine using an acetyl donor, acetyl coenzyme A (AcCoA), to generate UDP-2,4-diacetamido-2,4,6-trideoxy-β-L-altropyranose as an intermediate of pseudaminic acid synthesis (Fig. S1) [8]. Given that PseH mutants are devoid of flagellar filaments and hook structures and are, as a result, non-motile, the PseH-mediated acetylation step of O-linked glycosylation is critical for the formation of functional flagella in *C. jejuni* [15]. To date, PseH has not been structurally characterized, and thus, it is still unknown how PseH recognizes its cofactor and substrate for the acetylation reaction. Moreover, given that the first two steps, dehydration and amination, in both the *C. jejuni* O- and N-linked glycosylation pathways are mediated by homologous enzymes with similar structural folds, it would be interesting to examine whether the third enzyme, PseH, also shares structural and biochemical properties with the acetyltransferase PglD of the *C. jejuni* N-linked glycosylation pathway [6,7,13,14]. Here, we report the crystal structures of *C. jejuni* PseH alone (cjPseH) and in complex with AcCoA (cjPseH^{AcCoA}), which highlight the structural features and enzymatic mechanism of cjPseH that are distinct from other glycosylation-associated acetyltransferases.

2. Materials and methods

2.1. Protein expression and purification

A cjPseH expression vector was constructed, and recombinant cjPseH protein was expressed and purified as described elsewhere [16]. Briefly, the PseH-encoding gene was amplified by PCR and ligated into a modified pET49b expression vector to express cjPseH protein appended to an N-terminal His_6 tag and a thrombin cleavage site. cjPseH protein expression was induced by 1 mM IPTG at 18 °C overnight using *E. coli* BL21 (DE3) cells. The recombinant cjPseH protein was first purified by Ni-NTA affinity chromatography of the cell lysate and eluted using 250 mM imidazole. The resultant eluate was incubated with thrombin to remove the N-terminal His_6 tag. The digested cjPseH protein was further purified by cation-exchange chromatography using a Mono S 10/100 column and then by gel-filtration chromatography using a Superdex 200 16/600 column.

2.2. Crystallization and X-ray diffraction

cjPseH crystals were produced at 18 °C by the sitting-drop vapor-diffusion method in 1 μl drops consisting of 0.5 μl of cjPseH protein solution (15 mg/ml cjPseH, 150 mM NaCl, 5 mM β-mercaptoethanol, 20 mM HEPES, pH 7.4) and 0.5 μl of reservoir solution (22–24% PEG MME 550, 4 mM reduced glutathione, 4 mM oxidized glutathione, 0.1 M phosphate-citrate, pH 4.4–4.6 or 28% PEG 300, 10 mM β-mercaptoethanol, 0.1 M phosphate-citrate, pH 4.4). To obtain cjPseH^{AcCoA} crystals, cjPseH crystals grown in 28% PEG 300, 10 mM β-mercaptoethanol, 0.1 M phosphate-citrate, pH 4.4 were incubated in the presence of 10 mM AcCoA for 10 h. Crystals in PEG MME 550 solutions were cryo-protected by 20–25% glycerol and flash-cooled at −173 °C. Crystals in PEG 300 solutions were directly frozen in a cryo-stream without the addition of extra cryo-protectants. X-ray diffraction data for cjPseH and cjPseH^{AcCoA} were collected at beamlines 5C and 7A of the Pohang Accelerator Laboratory, respectively. The diffraction data were reduced and scaled using the HKL2000 package [17]. X-ray diffraction statistics are shown in Table S1.

2.3. Structure determination

The cjPseH structure was determined by molecular replacement with the PHASER program using a search model of spermidine N-acetyltransferase SpeG (PDB ID 4JJX) [18]. The cjPseH model was completed by iterative model building and refinement using the COOT and REFMAC5 programs, respectively [19,20]. The cjPseH^{AcCoA} structure was solved by molecular replacement using the refined cjPseH structure as a search model. An AcCoA molecule was clearly identified as strong positive electron density in the initial difference map. The final cjPseH^{AcCoA} model was achieved by several rounds of model building and refinement. The structure refinement statistics are shown in Table S1.

3. Results and discussion

3.1. The overall structure of cjPseH

The cjPseH and cjPseH^{AcCoA} crystal structures were determined by molecular replacement and refined to R_{free}s of 23.3% and 22.9%, respectively, at 1.95 Å resolution (Table S1). Because the two structures are essentially identical, the more stabilized cjPseH^{AcCoA} structure will be mainly described unless otherwise noted. The final cjPseH^{AcCoA} model includes 141 residues (residues 1–22 and 32–150) across the entire cjPseH protein (residues 1–157) (Figs. 1 and 2). Nine residues (residues 23–31) of the α1–α2 loop and seven C-terminal residues (residues 151–157) were not visible in the electron density map, presumably due to high flexibility, and were not built into the final model of cjPseH^{AcCoA}.

cjPseH adopts a single domain structure of a canonical GNAT fold with a central β-sheet of seven β-strands (β1–β7) decorated by four α-helices (α1–α4) (Fig. 1A and B). The single domain structure can be subdivided into two lobes, the N-lobe (β1-α1-α2-β2-β3-β4-α3) and C-lobe (β5-α4-β6-β7), by splaying β4- and β5-strands that make main-chain hydrogen bonds (H-bonds) with each other only in their N-terminal regions and are separated at their C-terminal segments to accommodate AcCoA. The surface of the cjPseH structure features two continuous grooves, groove-A and groove-S (Fig. 1C). The deep, narrow groove-A is walled by β4 and β5, and provides the AcCoA binding site (see Section 3.2). The shallow, wide groove-S is supported on the bottom by the β3 and β4 strands, and is buttressed by α1, α2, and β5. The groove-S seems to be involved in substrate recruitment (see Section 3.3). The two grooves are bridged in the middle of β4, presumably providing an engagement

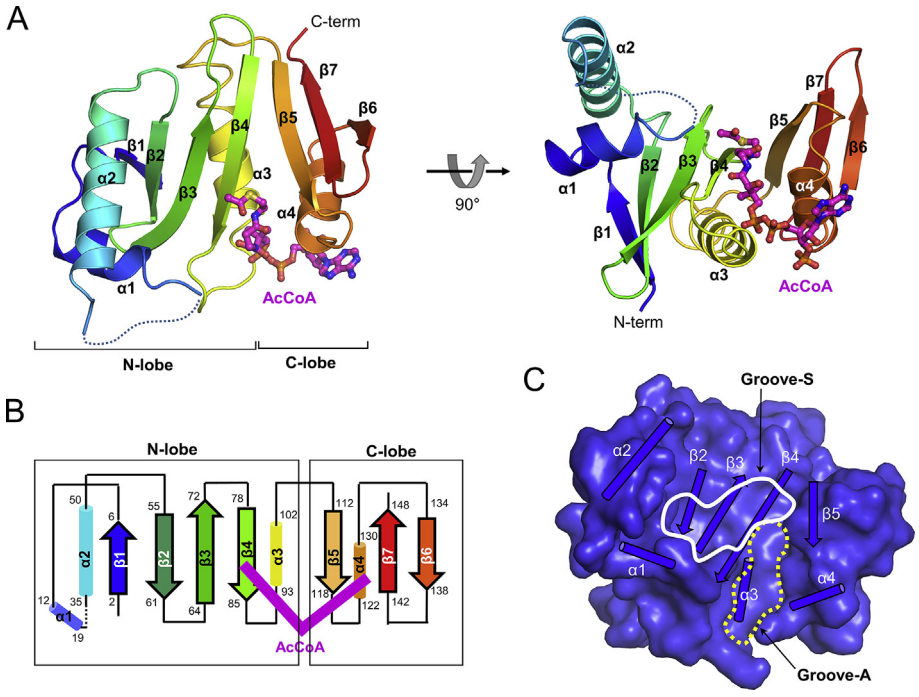

Fig. 1. The cjPseH structure and its grooves. (A) The overall structure of cjPseH^{AcCoA} in a ribbon diagram rainbow-colored from blue at the N-terminus to red at the C-terminus. AcCoA is depicted by a ball-and-stick model (carbon, magenta; oxygen, red; nitrogen, blue; phosphorus, orange; sulfur, yellow). The disordered region (residues 23–31) of the α1–α2 loop is represented by dotted lines. (B) Schematic diagrams for the secondary structures of cjPseH^{AcCoA}. α-helices and β-strands are shown by rods and arrows, respectively. The boundary residues of each secondary structure are numbered. AcCoA is represented by magenta sticks. (C) cjPseH groove-A and groove-S. cjPseH is shown in blue surfaces with groove-forming secondary structures (α-helices, rods; β-strands, arrows). Groove-A and groove-S are outlined by dotted yellow and solid white lines, respectively. (For interpretation of the references to color in this figure legend, the reader is referred to the web version of this article.)

point between the acetyl donor and the acceptor during the enzymatic reaction of cjPseH.

cjPseH is a small, compact GNAT acetyltransferases with 157 residues that lacks the additional domain and the N-terminal β-strand, β0, observed in other GNAT enzymes. Moreover, cjPseH was monomeric in solution, based on gel filtration chromatography analysis (Fig. S2). Consistently, the asymmetric unit of cjPseH crystals contained one cjPseH molecule with no significant homotypic binding interfaces generated by crystallographic symmetry. The unique monomeric nature of cjPseH contrasts with the dimeric assembly of many GNAT enzymes, such as spermidine N1-acetyltransferase, TDP-fucosamine acetyltransferase, and aminoglycoside N-acetyltransferase [21–23].

Dali server searches indicated that the cjPseH structure does not resemble any acetyltransferases associated with protein glycosylation, such as *C. jejuni* PglD. Instead, cjPseH exhibited the highest structural similarity with spermidine N-acetyltransferase (PDB ID 4MHD) from *Vibrio cholerae* with a root mean square deviation (RMSD) value of 1.5 Å (132 Cα atoms), although their substrates are completely different (Fig. S3). Among other GNAT structures, cjPseH was enzymatically related to the *E. coli* TDP-fucosamine acetyltransferase, WecD (PDB ID 2FT0), because both acetylate

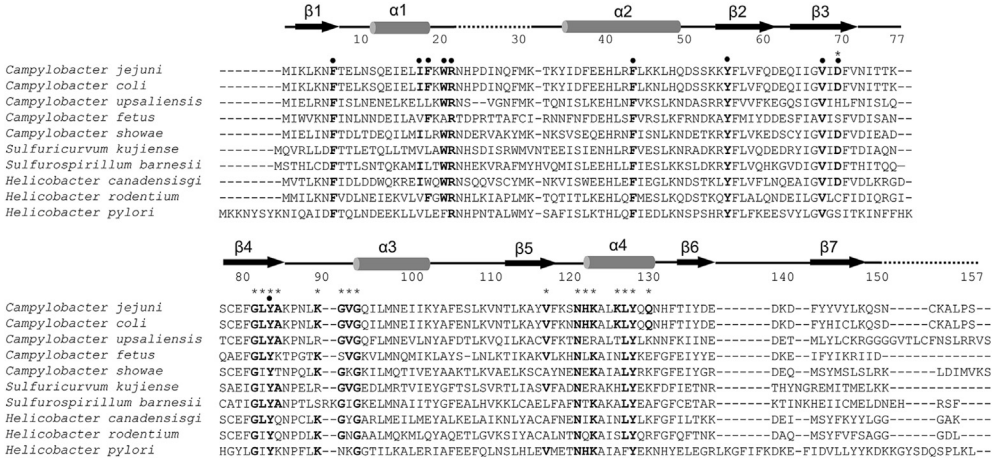

Fig. 2. The amino sequence alignment of cjPseH and its orthologs in ε-proteobacteria. The AcCoA-binding residues and the putative substrate-binding residues are indicated by stars and dots above the cjPseH sequence, respectively, and are shown in bold along with identical residues of cjPseH's orthologs. The secondary structural elements (α-helices, rods; β-strands, arrows) of cjPseH are shown above the sequence alignment, and the cjPseH residues that are missing in the cjPseH^{AcCoA} structure are designated by dotted lines.

nucleotide-linked sugars (Fig. S3) [22]. Comparing the cjPseH and WecD structures revealed an RMSD value of 2.4 Å (109 Cα atoms) and 16% sequence identity. Although cjPseH, spermidine N-acetyltransferase, and WecD adopt similar overall structures, significant structural differences were observed at or near two of the loops, the α1–α2 loop and the β6–β7 loop. The structural differences appear to be responsible for substrate specificity and variations in inter-subunit or inter-domain interactions.

3.2. cjPseH binding to AcCoA

The groove-A is formed between the N-lobe (the α1–α2 loop, β4, the β4–α3 loop, and α3) and C-lobe (β5, the β5–α4 loop, and α4), and holds one AcCoA molecule (Fig. 3A and B). The groove-A appears to be pre-configured to accommodate AcCoA because cjPseH does not undergo substantial structural rearrangements upon AcCoA binding (RMSD, 0.26 Å for 140 Cα atoms). Minor changes are made in the side-chain conformers of L83 and its neighboring M97 to avoid steric clashes between AcCoA and L83 (Fig. S4). Despite the lack of major positional displacements of cjPseH residues, AcCoA binding stabilizes residues in the β4–α3 and β5–α4 loops and their neighboring residues in the β6–β7 loop as indicated by substantial decreases in the temperature B-factors of the Cα atoms up to 22 $Å^2$ after AcCoA binding (average B-factor decrease, 3.5 $Å^2$) (Fig. 3C and S5).

The AcCoA molecule bound to cjPseH is shaped like the letter 'L' and wraps α4 along its helical axis (Fig. 3A and B). AcCoA consists of three parts, including the acetyl group, pantetheine, and 3′-phosphate ADP (Fig. S1B). The acetyl group and the pantetheine moiety form the vertical part of the L-shape with the acetyl end directed into groove-S. The pantetheine moiety is well buried in groove-A. The pyrophosphate group of the 3′-phosphate ADP moiety makes a perpendicular turn to form the corner of the L-shaped AcCoA between the pantetheine moiety and ADP's adenosine group. The adenosine group and its linked 3′-phosphate group face PseH α4 on one side but are exposed to the bulk solvent on the other side.

AcCoA is deeply inserted into the groove-A between the two splaying β-strands, N-lobe β4 and C-lobe β5, and makes diverse interactions, including H-bonds, a salt bridge, hydrophobic interactions, and van der Waals interactions, with highly conserved PseH residues with a buried surface area of ~490 $Å^2$ (Fig. 3B and S6). The pantetheine moiety and pyrophosphate group of AcCoA contribute to a majority of these interactions (Fig. 3B). The pantetheine moiety makes hydrophobic interactions with β4 L83, β5 V117 and α4 L127, and H-bonds with the main chains of β4 L83 and A85 and the side chain of N121 in the β5–α4 loop. The pyrophosphate group of the 3′-phosphate ADP moiety is enclosed by the β4–α3 loop and α4, and is clasped by two lysine residues, K90 and K123, on the top. The pyrophosphate group makes four H-bonds and one salt bridge with the main chain nitrogen atoms of G91, V92, and G93 and the side chain of K90, respectively. These extensive interactions with the groove-A residues stabilize the pantetheine moiety and pyrophosphate group as indicated by their low B-factors (Fig. 3C). In contrast, the adenosine group of the 3′-phosphate ADP moiety exhibited the highest flexibility potentially due to its lack of specific interactions and exposure to solution, although its linked 3′-phosphate group makes three H-bonds with the side chain of α4 Q130. Consistently, the structural positions of the adenine groups in other GNAT enzymes are highly variable. Taken together, the pantetheine and pyrophosphate groups seem to play a key role in optimally positioning AcCoA in the groove-A.

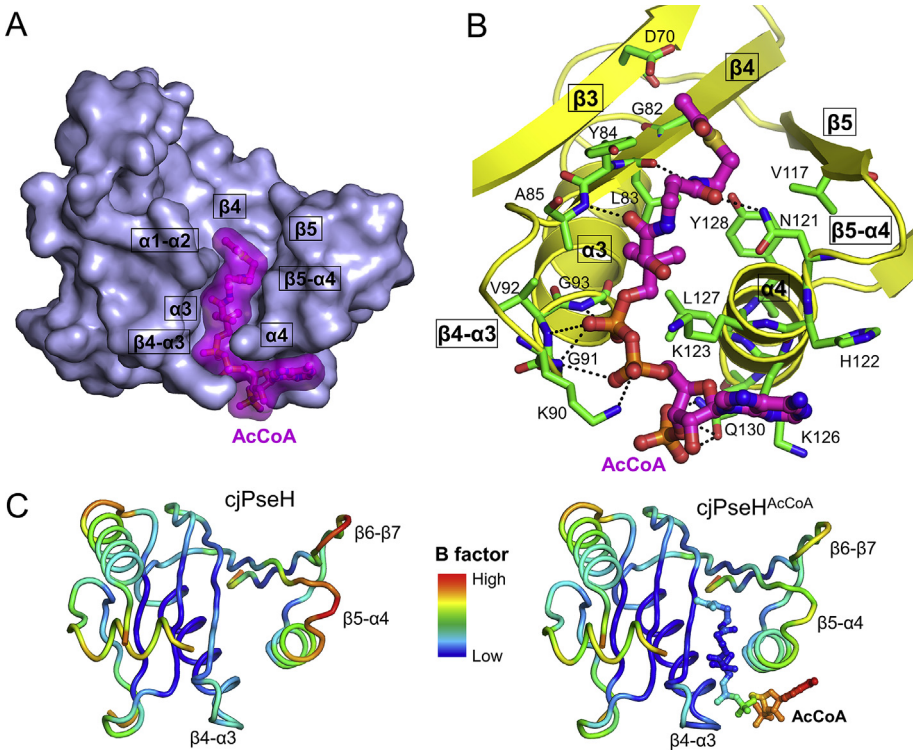

Fig. 3. The AcCoA-binding site of cjPseH. (A) AcCoA binding to the cjPseH groove-A. AcCoA is shown as a magenta ball-and-stick model with surface representation, and cjPseH is depicted in light blue surface. (B) The cjPseH-AcCoA interaction. cjPseH is traced in yellow ribbons and the AcCoA-binding residues are shown as green sticks. AcCoA is depicted as a ball-and-stick model (carbon, magenta; oxygen, red; nitrogen, blue; phosphorus, orange; sulfur, yellow). H-bonds and a salt bridge are represented by dotted lines. (C) Temperature B-factor analysis of the cjPseH (left) and cjPseH^{AcCoA} (right) structures. The B-factors of the cjPseH Cα atoms (coils) and AcCoA atoms (a ball-and-stick model) are color-coded from blue for low B-factors to red for high B-factors. (For interpretation of the references to color in this figure legend, the reader is referred to the web version of this article.)

3.3. Implication of the cjPseH structure in substrate binding and enzymatic catalysis

Each GNAT enzyme interacts with its specific substrate by engaging various structural elements from the N-lobe (α1, α2, the α1–α2 loop, and β4) and C-lobe (β5, the β5–α4 loop, the extended β6–β7 arm), or even by involving additional domains and subunits on the side of the C-lobe. Such structural variations contribute to the substrate specificity of each GNAT but make it difficult to understand substrate-recognition modes and catalytic mechanisms unless GNAT-substrate structures are available. In this regard, our cjPseH^{AcCoA} structure provides valuable information about substrate binding and catalysis.

The cjPseH groove-S is created predominantly by the N-lobe (α1, α2, the α1–α2 loop, β2, β3, and β4) with a small contribution from C-lobe β5 (Fig. 1C), and is highly likely to be responsible for substrate association for the following reasons. First, the acetyl group of AcCoA is located in the joining point of groove-A and groove-S, and points toward the open space in groove-S (Fig. 4A). Second, two entities of extra electron density were found that presumably serve as pseudosubstrates inside the groove-S in the N-lobe (Fig. 4). The smaller electron density resides next to the acetyl group with a distance of 3.5 Å. The larger electron density is curved along the cavity surface and located at a distance of 7 Å from the acetyl group. The electron density is surrounded by ten cjPseH residues (F7, I18, F19, W21, R22, F44, Y56, V68, D70, and Y84) that are highly conserved in cjPseH's orthologs with an average sequence identity of 81% (Figs. 2 and 4). Therefore, we propose that the groove-S that is mainly positioned in the N-lobe would function as the substrate-binding site of cjPseH. The contribution of the N-lobe may be enhanced by its highly flexible α1–α2 loop of N-lobe as in *Mycobacterium tuberculosis* aminoglycoside 2′-N-acetyltransferase [23]. Consistent with the proposed major role of the N-lobe in substrate binding, the contribution of the C-lobe side seems to be minimal because cjPseH is a single-domain monomeric protein that does not require binding partners or additional domains and possesses a substantially short β6–β7 arm.

GNAT enzymes have been proposed to drive acetyl transfer reaction through a direct nucleophilic attack of the amino group of the substrate on the thioester carbon of AcCoA [24]. The direct acetyl transfer mechanism involves a general base and a general acid. A general base deprotonates the amino group of the substrate to facilitate the nucleophilic attack, and a general acid protonates and stabilizes the thiolate anion generated after collapse of the tetrahedral AcCoA-substrate intermediate. Our structural analysis of the chemical environment around the acetyl group of AcCoA, combined with sequence conservation analysis, allowed us to propose key residues of the acetyl transfer mechanism. cjPseH Y128 potentially functions as a general acid, as in *M. tuberculosis* aminoglycoside 2′-N-acetyltransferase, given that the hydroxyl group of the absolutely conserved tyrosine residue, Y128, is located only 4.4 Å from the sulfur atom of AcCoA (Figs. 2 and 3B, and S7) [23]. However, there is no obvious candidate for a general base, such as a glutamate residue, in cjPseH near the acetyl end of AcCoA. Instead, deprotonation of the amino group may occur though a water molecule that H-bonds to the carboxylic group of an aspartate residue, D70, as proposed for *Salmonella enterica* aminoglycoside 6′-N-acetyltranserase [25].

3.4. cjPseH is a unique acetyltransferase involved in bacterial protein glycosylation

To date, only one class of acetyltransferases has been structurally characterized in bacterial protein glycosylation pathways, and this class includes *C. jejuni* PglD (cjPglD) of the N-glycosylation pathway and the acetyltransferase domain of the *N. gonorrhoeae* bifunctional PglB enzyme (ngPglB-ACT) that functions in O-glycosylation [26,27]. Although, like cjPglD and ngPglB-ACT, cjPseH acetylates the 4-amino group on UDP-4-amino-sugar substrates (UDP-4-amino-4,6-dideoxy-N-acetyl-β-L-altrosamine for cjPseH and UDP-2-acetamido-4-amino-2,4,6-trideoxy-α-D-glucopyranose for cjPglD and ngPglB-ACT) using AcCoA, cjPseH is completely different from cjPglD and ngPglB-ACT in its structural architecture, oligomeric status, and AcCoA- and substrate-binding modes. cjPglD and ngPglB-ACT assemble into homotrimers, each subunit of which exhibits a two-domain structure with an N-terminal β-α-β-α-β-α Rossman-like domain and a C-terminal left-handed β-helix domain. cjPseH, on the other hand, is monomeric with a one-domain structure (Fig. S8). The cjPglD homotrimer positions AcCoA and a substrate in an 'L'-shaped deep groove between two subunits. However, cjPseH forms a deep groove and a shallow groove on the monomeric surface potentially to accommodate

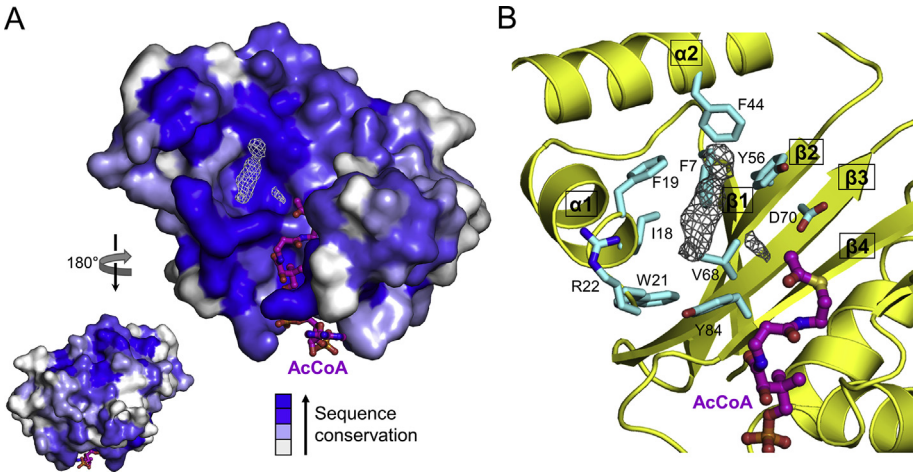

Fig. 4. The potential substrate-binding site of cjPseH in groove-S. (A) Additional electron density (white wires; 3 σ level of F_o-F_c map) inside groove-S in the proximity of the AcCoA acetyl group. cjPseH is represented by surfaces color-coded in a gradient from blue for highly conserved residues to white for poorly conserved residues. Protein sequence conservation was calculated by the ConSurf server on the basis of the sequence alignment shown in Fig. 2 [28]. (B) The potential substrate-binding residues (cyan sticks) of cjPseH (yellow ribbons). The additional electron density in groove-S is shown by gray wires, and AcCoA is depicted as a ball-and-stick model. (For interpretation of the references to color in this figure legend, the reader is referred to the web version of this article.)

AcCoA and substrate. Overall, the cjPseH structure represents a new class of acetyltransferase that has not been described in bacterial protein glycosylation.

In conclusion, our structural studies are of significance in demonstrating that cjPseH with the GNAT fold contains two grooves that play a key role in acetyl transfer using a distinct mechanism from other glycosylation-associated acetyltransferases. To reveal the exact catalytic mechanism of cjPseH and design cjPseH-specific antibiotic inhibitors, future structural studies on the cjPseH-substrate interaction and cjPseH's acetylation mechanism are required.

Data deposition

The atomic coordinates and structure factors for cjPseH (PDB ID 4XPK) and its complex with acetyl coenzyme A (PDB ID 4XPL) have been deposited in the Protein Data Bank, www.pdb.org.

Conflict of interest

The authors declare that there are no conflicts of interest.

Acknowledgments

X-ray diffraction datasets were collected at beamlines 5C and 7A of the Pohang Accelerator Laboratory (Republic of Korea). This study was supported by Basic Science Research Program through the National Research Foundation of Korea (NRF) funded by the Ministry of Education (2014R1A1A2053497 to SIY).

Transparency document

Transparency document related to this article can be found online at http://dx.doi.org/10.1016/j.bbrc.2015.02.041.

Appendix A. Supplementary data

Supplementary data related to this article can be found at http://dx.doi.org/10.1016/j.bbrc.2015.02.041.

References

[1] A. Neuberger, Carbohydrates in protein: the carbohydrate component of crystalline egg albumin, Biochem. J. 32 (1938) 1435–1451.
[2] E. Weerapana, B. Imperiali, Asparagine-linked protein glycosylation: from eukaryotic to prokaryotic systems, Glycobiology 16 (2006) 91R–101R.
[3] H. Nothaft, C.M. Szymanski, Protein glycosylation in bacteria: sweeter than ever, Nat. Rev. Microbiol. 8 (2010) 765–778.
[4] B. Jeon, W.T. Muraoka, Q. Zhang, Advances in Campylobacter biology and implications for biotechnological applications, Microb. Biotechnol. 3 (2010) 242–258.
[5] J.J. Gilbreath, W.L. Cody, D.S. Merrell, D.R. Hendrixson, Change is good: variations in common biological mechanisms in the epsilonproteobacterial genera Campylobacter and Helicobacter, Microbiol. Mol. Biol. Rev. 75 (2011) 84–132.
[6] I.C. Schoenhofen, D.J. McNally, E. Vinogradov, D. Whitfield, N.M. Young, S. Dick, W.W. Wakarchuk, J.R. Brisson, S.M. Logan, Functional characterization of dehydratase/aminotransferase pairs from Helicobacter and Campylobacter: enzymes distinguishing the pseudaminic acid and bacillosamine biosynthetic pathways, J. Biol. Chem. 281 (2006) 723–732.
[7] N.B. Olivier, M.M. Chen, J.R. Behr, B. Imperiali, In vitro biosynthesis of UDP-N,N′-diacetylbacillosamine by enzymes of the *Campylobacter jejuni* general protein glycosylation system, Biochemistry 45 (2006) 13659–13669.
[8] I.C. Schoenhofen, D.J. McNally, J.R. Brisson, S.M. Logan, Elucidation of the CMP-pseudaminic acid pathway in *Helicobacter pylori*: synthesis from UDP-N-acetylglucosamine by a single enzymatic reaction, Glycobiology 16 (2006) 8C–14C.
[9] P. Thibault, S.M. Logan, J.F. Kelly, J.R. Brisson, C.P. Ewing, T.J. Trust, P. Guerry, Identification of the carbohydrate moieties and glycosylation motifs in *Campylobacter jejuni* flagellin, J. Biol. Chem. 276 (2001) 34862–34870.
[10] C.G. Zampronio, G. Blackwell, C.W. Penn, H.J. Cooper, Novel glycosylation sites localized in *Campylobacter jejuni* flagellin FlaA by liquid chromatography electron capture dissociation tandem mass spectrometry, J. Proteome Res. 10 (2011) 1238–1245.
[11] W.K. Chou, S. Dick, W.W. Wakarchuk, M.E. Tanner, Identification and characterization of NeuB3 from *Campylobacter jejuni* as a pseudaminic acid synthase, J. Biol. Chem. 280 (2005) 35922–35928.
[12] E.S. Rangarajan, A. Proteau, Q. Cui, S.M. Logan, Z. Potetinova, D. Whitfield, E.O. Purisima, M. Cygler, A. Matte, T. Sulea, I.C. Schoenhofen, Structural and functional analysis of *Campylobacter jejuni* PseG: a udp-sugar hydrolase from the pseudaminic acid biosynthetic pathway, J. Biol. Chem. 284 (2009) 20989–21000.
[13] I.C. Schoenhofen, V.V. Lunin, J.P. Julien, Y. Li, E. Ajamian, A. Matte, M. Cygler, J.R. Brisson, A. Aubry, S.M. Logan, S. Bhatia, W.W. Wakarchuk, N.M. Young, Structural and functional characterization of PseC, an aminotransferase involved in the biosynthesis of pseudaminic acid, an essential flagellar modification in *Helicobacter pylori*, J. Biol. Chem. 281 (2006) 8907–8916.
[14] N. Ishiyama, C. Creuzenet, W.L. Miller, M. Demendi, E.M. Anderson, G. Harauz, J.S. Lam, A.M. Berghuis, Structural studies of FlaA1 from *Helicobacter pylori* reveal the mechanism for inverting 4,6-dehydratase activity, J. Biol. Chem. 281 (2006) 24489–24495.
[15] P. Guerry, C.P. Ewing, M. Schirm, M. Lorenzo, J. Kelly, D. Pattarini, G. Majam, P. Thibault, S. Logan, Changes in flagellin glycosylation affect Campylobacter autoagglutination and virulence, Mol. Microbiol. 60 (2006) 299–311.
[16] W.S. Song, S.I. Yoon, Crystal structure of FliC flagellin from *Pseudomonas aeruginosa* and its implication in TLR5 binding and formation of the flagellar filament, Biochem. Biophys. Res. Commun. 444 (2014) 109–115.
[17] Z. Otwinowski, W. Minor, Processing X-ray diffraction data collected in oscillation mode, Methods Enzymol. 276 (1997) 307–326.
[18] A.J. McCoy, R.W. Grosse-Kunstleve, P.D. Adams, M.D. Winn, L.C. Storoni, R.J. Read, Phaser crystallographic software, J. Appl. Crystallogr. 40 (2007) 658–674.
[19] P. Emsley, K. Cowtan, Coot: model-building tools for molecular graphics, Acta Crystallogr. D. Biol. Crystallogr. 60 (2004) 2126–2132.
[20] G.N. Murshudov, A.A. Vagin, E.J. Dodson, Refinement of macromolecular structures by the maximum-likelihood method, Acta Crystallogr. D. Biol. Crystallogr. 53 (1997) 240–255.
[21] E.J. Montemayor, D.W. Hoffman, The crystal structure of spermidine/spermine N1-acetyltransferase in complex with spermine provides insights into substrate binding and catalysis, Biochemistry 47 (2008) 9145–9153.
[22] M.N. Hung, E. Rangarajan, C. Munger, G. Nadeau, T. Sulea, A. Matte, Crystal structure of TDP-fucosamine acetyltransferase (WecD) from *Escherichia coli*, an enzyme required for enterobacterial common antigen synthesis, J. Bacteriol. 188 (2006) 5606–5617.
[23] M.W. Vetting, S.S. Hegde, F. Javid-Majd, J.S. Blanchard, S.L. Roderick, Aminoglycoside 2′-N-acetyltransferase from *Mycobacterium tuberculosis* in complex with coenzyme A and aminoglycoside substrates, Nat. Struct. Biol. 9 (2002) 653–658.
[24] M.W. Vetting, S.d.C. LP, M. Yu, S.S. Hegde, S. Magnet, S.L. Roderick, J.S. Blanchard, Structure and functions of the GNAT superfamily of acetyltransferases, Arch. Biochem. Biophys. 433 (2005) 212–226.
[25] M.W. Vetting, S. Magnet, E. Nieves, S.L. Roderick, J.S. Blanchard, A bacterial acetyltransferase capable of regioselective N-acetylation of antibiotics and histones, Chem. Biol. 11 (2004) 565–573.
[26] N.B. Olivier, B. Imperiali, Crystal structure and catalytic mechanism of PglD from *Campylobacter jejuni*, J. Biol. Chem. 283 (2008) 27937–27946.
[27] E.S. Rangarajan, K.M. Ruane, T. Sulea, D.C. Watson, A. Proteau, S. Leclerc, M. Cygler, A. Matte, N.M. Young, Structure and active site residues of PglD, an N-acetyltransferase from the bacillosamine synthetic pathway required for N-glycan synthesis in *Campylobacter jejuni*, Biochemistry 47 (2008) 1827–1836.
[28] A. Armon, D. Graur, N. Ben-Tal, ConSurf: an algorithmic tool for the identification of functional regions in proteins by surface mapping of phylogenetic information, J. Mol. Biol. 307 (2001) 447–463.